

## ROCK CHEMISTRY AND ALTERATION PROCESSES IN THE ALUTO-LANGANO GEOTHERMAL FIELD, ETHIOPIA

M. TEKLEMARIAM

Geological Survey of Ethiopia

**SUMMARY**- In the Aluto-Langano geothermal field, two types of alteration trends have been recognized using different chemical diagrams: argillic and propylitic. The rock samples from the lateral outflow zone show a pronounced alteration trend towards the phyllosilicate composition. This is in agreement with the common occurrence of chlorite, smectite, illite and other clay minerals in these rocks. On the other hand, a few samples show a different trend towards the calcite and epidote composition where a relict propylitic alteration is prominent in these rocks. The rock samples from the upflow zone depict alteration towards the calcite and epidote composition which is consistent with the propylitic alteration characterizing these rock samples. The upflow zone is characterized by waters with up to 14 ppb of Au and up to 3.4 ppb of Ag. These metals can be deposited in the zones of lateral flow.

### 1. INTRODUCTION

The Aluto Langano geothermal field is located about 200 Km South of Addis Ababa, close to the eastern margin of the Ethiopian Rift, and well inside the presently axis of the rift, i.e. the Wonji Fault Belt (WFB; Figure 1). It is a high temperature water dominated gas rich geothermal field hosted by peralkaline rhyolitic lavas and ignimbrites as well as transitional to alkaline basalts.

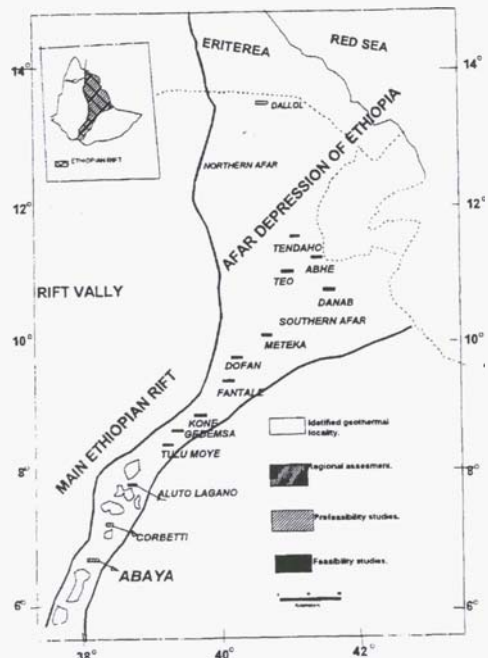


Fig.1 Location Map of the Geothermal Prospect Areas within the Ethiopian Rift Valley

In the Aluto-Langano geothermal field, eight deep exploratory wells were drilled. The maximum depth drilled is 2500m (LA-8) and the maximum temperature measured is 335°C (LA-6). Exploratory and production wells identified an upflow zone (wells LA-3 and LA-6) with

temperature of 300-335°C and PCO<sub>2</sub> of the order of 1.3 Mpa. The zone of lateral outflow is characterized by more diluted waters with temperature in the range of 150-270°C, local temperature inversion at the margins of the field and very high PCO<sub>2</sub> (2-6 Mpa). This geothermal field is currently at a stage of development where the four productive wells supply steam and brine to operate the pilot power plant. The main objective of the present work is to characterize the chemical changes caused by the passage of hydrothermal fluids, and to learn about mass transfer processes taking place in the reservoir.

### 2. GEOLOGY OF THE ALUTO-LANGANO AREA

At Aluto, except for some fluvio-lacustrine sediments, all outcropping rocks are volcanic (Figure 2). The outcropping units in the Aluto-Langano area mainly comprising the following: (a) Tertiary ignimbrite: is the oldest rock unit of the area outcropping on the main eastern Rift escarpment. Its K/Ar radiometric age resulted to be  $2.30 \pm 0.03$  Ma (Teklemariam, 1996). (b) Bofa basalt: is an outcrop on the eastern, northeastern and southern parts of the Aluto-volcanic complex. Its K/Ar age, determined by the present study, is  $1.6 \pm 0.5$  Ma (Teklemariam, 1996). (c) Lake sediments: these occur mainly along gorges and streams in the Aluto-Langano area but are widespread over large parts of the rift floor elsewhere. The age of these sediments has been estimated at 0.1 Ma (Laury and Albritton, 1975); (d) Aluto-Volcanic products: these products consist of a complex sequence of alternating pyroclastics that have a peralkali-rhyolitic composition. The oldest product is represented by the Hulo Seyno ignimbrite dated at  $155,000 \pm 8,000$  years by K/Ar method (ELC, 1986), while one of the youngest products (pantelleritic

obsidian) dated at 20,000 years using Fission track method (Teklemariam, 1996).

### 3. PETROLOGICAL RESULTS

The total alkali-silica diagram indicates that rocks of basaltic composition mostly fall in the field of alkaline basalt with a certain transitional tendency (Teklemariam, 1996). These fissural transitional to alkaline basalts are olivine-hypersthene normative; however some of them are slightly undersaturated with normative nepheline. In the  $\text{Al}_2\text{O}_3$  Vs  $\text{FeO}_T$  diagram, the silicic products of Aluto fall in the field of peralkaline rhyolite (pantellerite).

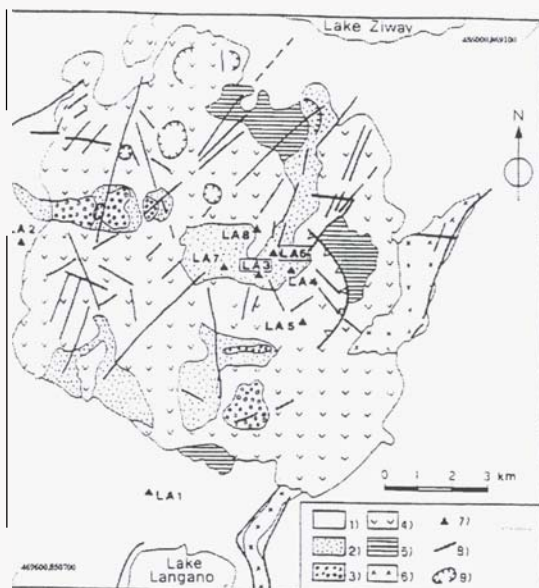


Figure 2. Simplified Geological map of the Aluto-Langano geothermal area with location of deep wells. (1) Recent Alluvium; (2) Peralkaline rhyolitic pyroclastics and lavas; (3) Obsidian flows; (4) Peralkaline rhyolite dome and tephra; (5) Hulo Seyno ignimbrite; (6) Bofa basalt; (7) Geothermal well; (8) Faults; (9) Volcanic center; (Modified after ELC, 1986).

### 4. HYDROTHERMAL ALTERATION AND CLAY MINERALOGY

In the upflow zone of the Aluto-Langano geothermal field (wells LA-3 and LA-6), the hydrothermal mineral assemblage is characterized by the presence of calc-silicate minerals such as epidote, garnet, prehnite and actinolite. However, these phases also occur as relics in wells where low temperatures are measured (wells LA-4, LA-7 and LA-8). Calcite, quartz, adularia, illite, pyrite, hematite and chlorite are widespread minerals in all wells both at low and high temperatures.

At Aluto, micaceous clay minerals and chloritic clays are the most abundant clay minerals, and

are sensitive to changes of temperature. Clay minerals were observed throughout the depths in all the wells. The distribution of clay mineral assemblages identified in the core samples from the deep wells as a function of temperature is described as follows. In the hottest part of the field (LA-3 and LA-6), the clay minerals are distributed into four distinct zones (Teklemariam et al., 1996): (i) Illite-smectite mixed layers ( $T < 170^\circ\text{C}$ ); (ii) Illite-Chlorite ( $170 < T < 310^\circ\text{C}$ ); (iii) Illite ( $310 < T < 320^\circ\text{C}$ ); and (iv) Chlorite ( $T > 320^\circ\text{C}$ ). However, in the wells drilled in the zone of lateral outflow the sequence of the clay mineral assemblages in order of increasing depth is characterized by (i) Illite-smectite mixed layers ( $T < 170^\circ\text{C}$ ); (ii) illite-chlorite ( $170 < T < 220^\circ\text{C}$ ); and (iii) chlorite-smectite mixed layers, vermiculite, chloritic intergrades and kaolinite at a temperature of  $< 220^\circ\text{C}$  and in the zones of temperature inversion.

### 5. FLUID CHEMISTRY AND SOLUTION-MINERAL EQUILIBRIA

The hot spring waters, and the fluid from temperature gradient (TG) and deep wells of the Aluto-Langano geothermal field belong to an alkali-bicarbonate chloride water, with pH near neutral to slightly alkaline (Mekuria et al., 1987; Gizaw, 1989; Teklemariam, 1996; Teklemariam and Beyene, 2000; 2001). The geothermal wells produce two phase fluid (water + steam) with a total flow rate of 10.4 – 25.6 Kg/sec. The deep wells in the upflow zone produce fluids of high enthalpy (1600-1650 kJ/Kg) while the wells along the outflow zone produce fluids with a lower enthalpy (1000 – 1250 kJ/Kg). The geothermal fluids are characterized by a high gas content of partial pressures of  $\text{CO}_2$  that can reach up to 60 bars (Gizaw, 1989; Teklemariam and Beyene, 2000; 2001).

The application of water-rock equilibria using Enthalpy-Chloride and  $\text{Na}/1000\text{-K}/100\text{-Mg}$  diagrams have demonstrated that none of the discharge waters can be taken as representative of the deep fluid in full equilibrium with the reservoir rock, and thus important mixing processes characterize even the hottest zone of the system.

### 6. MATERIALS AND METHODS USED

Fifty three altered rocks and recovered from the deep wells of Aluto-Langano (LA-1 to LA-8) and seven fresh outcropping rocks were analysed for major and trace elements in order to characterize the chemical changes caused by the passage of hydrothermal fluids and to learn about mass transfer processes taking place in the reservoir.

Major oxides and trace elements were analysed using X-ray fluorescence at the Department of Earth Sciences, University of Pisa. Chemical composition of selected minerals (illite, chlorite and epidote) and the stoichiometric composition of other minerals were analysed by Electron microprobe at the Department of Earth Sciences, University of Florence.

Drillcore samples, recovered from the deep wells of Aluto were analysed for trace metals (such as Au, Ag, Zn, Cu and Pb) using Atomic Absorption Spectrometer (AAS) with a graphite furnace. The geothermal fluids from wells LA-3, 6 and 8 were analysed for trace metals using AAS and Induced Coupled Plasma (ICP) at the Geochemical Laboratory of ENEL, Larderello Italy. Precipitates (encrustations) scraped from the silencer and/or separator of the wells LA-3, 6 and 8 were analysed for trace metals using Scanning Electron Microscope (SEM-EDS) and ICP-EDS at the Geochemical laboratory of U.S. Dept of Geological Survey, Reston, Virginia, U.S.A.

## 7. RESULTS

Representative chemical analysis of the core samples for major and trace elements from the deep wells of Aluto-Langano are given in Table 1. All the analysed core samples show significant alteration with a range of loss of ignition (LOI) **0.80-35.4**. Chemical analysis shows that the various alteration types have characteristic patterns of addition and removal of major and trace elements. Concentration of trace metals in the core samples from the deep wells of the Aluto-Langano geothermal field is presented in Table 2.

The chemical variation and alteration trends of the rhyolitic and basaltic rocks of Aluto-Langano have been described by using different chemical diagrams. These included: (a) the PF'-Al - KNC triangular diagram of de La Roche (1975); (b) the ACF and A'KF of Wrinkler (1974); and (c) the Isocon diagram of Grant (1986).

Table 1. Representative chemical analysis of the core samples for major oxides (wt%) and trace elements (ppm) from the deep wells of the Aluto-Langano geothermal field.

| Well                           | LA-3 | LA-3 | LA-4 | LA-4 | LA-6 | LA-7 | LA-8 |
|--------------------------------|------|------|------|------|------|------|------|
| Depth (m)                      | 1549 | 2000 | 1001 | 2095 | 1764 | 798  | 1050 |
| SiO <sub>2</sub>               | 46.6 | 74.7 | 34.1 | 71.1 | 74.9 | 69.6 | 48.9 |
| TiO <sub>2</sub>               | 2.8  | 0.2  | 1.21 | 0.53 | 0.19 | 0.56 | 2.73 |
| Al <sub>2</sub> O <sub>3</sub> | 17.4 | 11.6 | 11.2 | 12.9 | 12.7 | 12.7 | 16.3 |
| Fe <sub>2</sub> O <sub>3</sub> | 4.15 | 0.04 | 0.00 | 2.6  | 0.83 | 1.37 | 0.00 |
| FeO                            | 9.41 | 0.73 | 6.01 | 0.11 | 1.42 | 4.18 | 13.9 |
| MnO                            | 0.16 | 0.05 | 0.15 | 0.11 | .07  | 0.22 | 0.16 |
| MgO                            | 5.38 | 0.32 | 2.02 | 0.68 | .36  | 0.52 | 1.55 |
| CaO                            | 4.01 | 0.15 | 4.42 | 1.38 | .14  | 0.6  | 4.85 |
| Na <sub>2</sub> O              | 5.32 | 3.78 | 3.9  | 4    | 3.52 | 1.85 | 5.19 |
| K <sub>2</sub> O               | 0.97 | 4.57 | 1.33 | 4.72 | 5.51 | 6.27 | 0.74 |
| P <sub>2</sub> O <sub>5</sub>  | 0.4  | 0.01 | 0.74 | 0.08 | 0.01 | 0.07 | 1.76 |
| LOI                            | 5.32 | 2.31 | 35.4 | 1.2  | 0.80 | 1.94 | 5.33 |
| Rb                             | 21   | 4    | 30   | 103  | 113  | 140  | 18   |
| Sr                             | 343  | 24   | 430  | 83   | 27   | 32   | 494  |
| Zr                             | 203  | 859  | 230  | 721  | 888  | 797  | 437  |
| Ba                             | 349  | 160  | 571  | 339  | 197  | 377  | 441  |
| Ni                             | 19   | 1    | 4    | 4    | 1    | 2    | 5    |
| Cr                             | 51   | 2    | 3    | 18   | 3    | 3    | 9    |
| La                             | 16   | 83   | 36   | 77   | 39   | 104  | 60   |
| Ce                             | 48   | 124  | 75   | 146  | 132  | 195  | 122  |
| V                              | 311  | 3    | 56   | 20   | 3    | 11   | 172  |

Table 2. Concentration of trace metals in core samples from the deep wells of Aluto-Langano.

| SAMPLE         | Zn    | Cu    | Pb    | Ag    | Au    |
|----------------|-------|-------|-------|-------|-------|
| Well/Depth (m) | (ppb) | (ppm) | (ppm) | (ppb) | (ppb) |
| LA-3/850       | 108.3 | 27.7  | 12.1  | 75.5  | 5     |
| LA-3/1150      | 113.3 | 2.3   | 23.6  | 38.1  | 26    |
| LA-3/1449      | 104.7 | 10    | 15.6  | 73    | <4    |
| LA-3/1779      | 150.5 | 11.5  | 23.3  | <30   | 5     |
| LA-4/615       | 157   | 34.7  | 12    | 67.3  | 29    |
| LA-4/1001      | 147.2 | 2     | 12    | 74.9  | 43    |
| LA-4/2095      | 102.4 | 4.8   | 28.1  | 35.7  | 7     |
| LA-6/940       | 115   | 11    | 22.3  | 36    | 10    |
| LA-6/2200      | 278.3 | 19.8  | 66.3  | 241   | <4    |
| LA-7/550       | 134.7 | 1.5   | 16    | 37.4  | 11    |
| LA-7/1798      | 149   | 6.3   | 10.4  | <30   | 131   |
| LA-7/1791      | 115.9 | 4.8   | 15.5  | <30   | 176   |
| LA-7/2040      | 122.9 | 3.1   | 12.6  | 39.4  | 305   |
| LA-8/784       | 134.1 | 5     | 46.2  | 149   | 161   |
| LA-8/1050      | 197.4 | 18    | 15.8  | 74    | 108   |
| LA-8/2500      | 163.7 | 93.3  | 32.7  | 127.7 | 19    |

### 7.1 The PF'-Al-KNC triangular diagram

This triangular diagram is utilized in order to show the chemical behaviour of the pyroclastic rocks under process of hydration and hydrolysis. The rocks show the two alteration trends. The

chemical variables used in constructing this diagram are:

$$PF' = (1000/27) (Loss on ignition (LOI) + Fe_2O_3/10)^* 100 \text{ (in wt %)}$$

$$KNC = (K + Na + 2Ca)^* 100 \text{ (in milliatoms)}$$

$$Al = (5/3) Al^* 100 \text{ (in milliatoms)}$$

Thus, the chemical data from the Aluto-Langano wells were computed using these chemical variables and plotted on this diagram (Fig. 3). Aside from the chemical data of 53 rock samples, the diagram also presents the chemical composition of selected minerals (illite, chlorite and epidote) analysed by microprobe as well as the stoichiometric composition of other minerals.

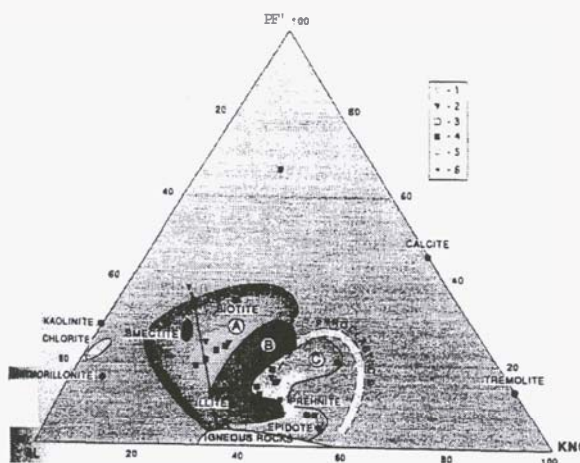


Figure 3. PF'-Al-KNC diagram (de La Roche, 1975) for the rocks of Aluto-Langano; (1) Unaltered peralkaline rhyolitic lavas and ignimbrite; (2) hydrothermally altered peralkaline rhyolitic lavas and ignimbrite; (3) Unaltered basalt (Bofa basalts); (4) altered basalt (Bofa basalts); (5) Altered lake sediment; (6) Altered volcano sediment. Field A and C = Lateral outflow zone; Field (B) = Upflow zone of the geothermal field.

The arrow in figure 3 indicates the hydrolysis and hydration of the rock forming minerals. The dispersion of samples towards the PF' and Al apexes indicates an argillic alteration, whereas a scattering of data towards the KNC apex indicates a propylitic alteration. In particular, the samples from the lateral outflow zone (Field A in figure 3) show a pronounced alteration trend towards the phyllosilicate compositions. This is in agreement with the common occurrence of chlorite, smectite, illite and other clay minerals in these rocks. On the other hand, a few samples show a different trend towards the calcite and epidote compositions (field C); in these samples a relict propylitic alteration is present. The samples from the upflow zone (field B in figure 3) show two different trends, towards the calcite and epidote

composition respectively. This is consistent with the propylitic alteration characterizing these rock samples.

## 7.2 The ACF and A'KF diagrams

The ACF diagram is utilized to represent graphically different mineral assemblages that occur in rocks of various compositions and within a limited range of metamorphic conditions. This diagram is mostly useful to show mineral paragenesis of calcium rich Ca, Al, Mg and Fe minerals, i.e. minerals occurring in metamorphic marls and mafic rocks (Wrinkler, 1974). The scheme for calculating the ACF ratios may be summarized as follows:

$$A = (Al_2O_3) + (Fe_2O_3) - (Na_2O) + (K_2O)$$

$$C = (CaO) - 3.3 (P_2O_5)$$

$$F = (MgO) + (MnO) + (FeO)$$

$$A + C + F = 100$$

The chemical data for fresh and altered rhyolitic and basaltic rock samples of Aluto-Langano were plotted on this diagram (Fig. 4a). In such a case, the mafic rocks (basalt) exhibit two ignimbrites; (2) hydrothermally altered peralkaline rhyolitic lavas and ignimbrite; (3) Unaltered basalt (Bofa basalts); (4) altered basalt (Bofa basalts); (5) Altered lake sediment; (6) Altered volcano sediment.

**trends of alteration: argillic and propylitic types of alteration.** The basaltic rocks which exhibit argillic type of alteration are plotted towards the mineral assemblages of smectite, chlorite, as well as pyrophyllite, whereas basaltic rocks that indicate propylitic type of alteration are plotted towards mineral assemblages of calc-silicate minerals such as prehnite, epidote and garnet (Fig. 4a). On the other hand, the rhyolitic rocks show scattered behaviour without clear trend of alteration. However, some of the altered rhyolitic rocks manifest an alteration trend towards the field of clay mineral assemblages (smectite, pyrophyllite) and Fe-oxides (hematite and magnetite).

The A'KF diagram is used to represent graphically K-minerals (K-feldspars, muscovite, biotite) together with minerals containing (Mg, Fe and Al). Minerals containing Ca cannot be shown on this diagram (Fig. 4b). The general calculation scheme to construct this diagram is:

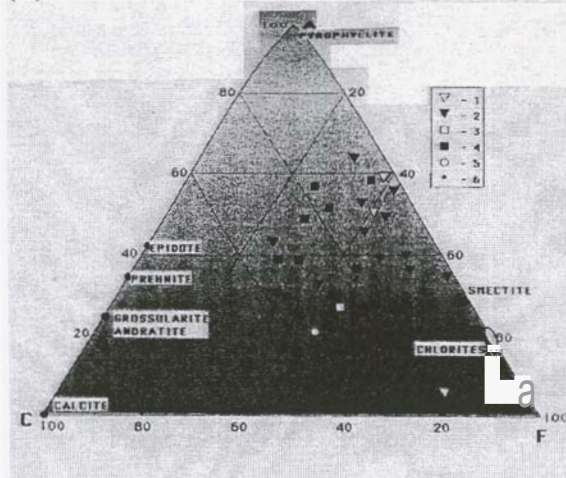
$$A' = (Al_2O_3) + (Fe_2O_3) - [(Na_2O) + (K_2O) + (CaO)]_2$$

$$K = K_2O$$

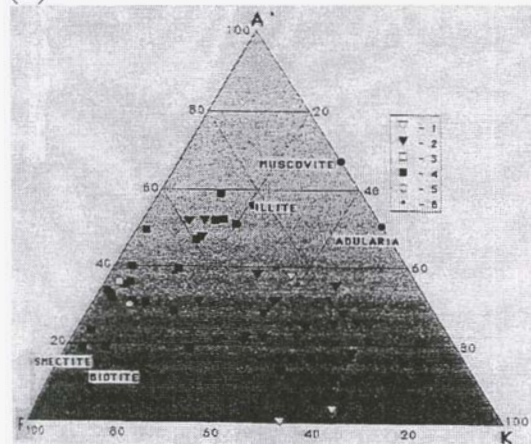
$$F = (FeO) + (MgO) + (MnO)$$

$$A' + K + F = 100$$

(A)



(B)



Figures 4. ACF diagram (A) and A'KF diagram (B) (Wrinkler, 1974) for the rocks of Aluto-Langano. (1) Unaltered peralkaline rhyolitic lavas and ignimbrite; (2) hydrothermally altered peralkaline rhyolitic lavas and ignimbrite; (3) Unaltered basalt (Bofa basalts); (4) altered basalt (Bofa basalts); (5) Altered lake sediment; (6) Altered volcano sediment.

The chemical data of basaltic rocks, computed using the above scheme, indicate an alteration trend towards the clay mineral assemblages, characterized by illite, smectite and biotite. On the other hand, the altered rhyolitic lavas and ignimbritic rocks are plotted towards K-feldspar end member. They exhibit an alteration process of K-metasomatism characterized by mineral assemblages of illite and adularia.

### 7.3 The isocon diagram

Comparison of the chemistry of the altered basaltic unit with unaltered outcrop of the Bofa basalt of similar composition and age was made using isocon diagram of Grant (1986). The plot in figure 5 shows the chemical composition of altered subsurface basalt as

compared to the composition of unaltered surface basaltic rock unit (Teklemariam, 1996).

The altered basaltic rocks show an increase in Na, Fe and H<sub>2</sub>O and depletion in K, Ca and Mg as well. A possible explanation is that the main alteration process occurred during alteration of the basaltic rocks are mainly Na-metasomatism (albitization) and hydration. Alteration processes, such as, albitization or Na-metasomatism could possibly be formed as a result of dissolution of the primary calcic plagioclase (anorthite-labradorite) minerals, and of replacement by sodium feldspars such as albite. The common occurrence of clay minerals such as illite and chlorite in the basaltic rock unit is mainly as a result of alteration processes of hydration and hydrolysis.

## 8. TRACE METAL CONCENTRATIONS IN ROCKS AND GEOTHERMAL FLUIDS

Drillcores from wells LA-3, 4, 6, 7 and 8 contain substantial amount of base metals such as Zn, Cu and Pb. Significant amount of Au (305 ppb) was found only in well LA-7, while similar amount of Ag was found mainly in wells LA-6 (241 ppb) and LA-8 (128 ppb). The high concentration of gold is particularly found within the highly altered peralkaline crystal rich ignimbrite (inferred to be the main productive horizon) in association with alteration mineral assemblages of quartz, calcite, pyrite, illite and adularia.

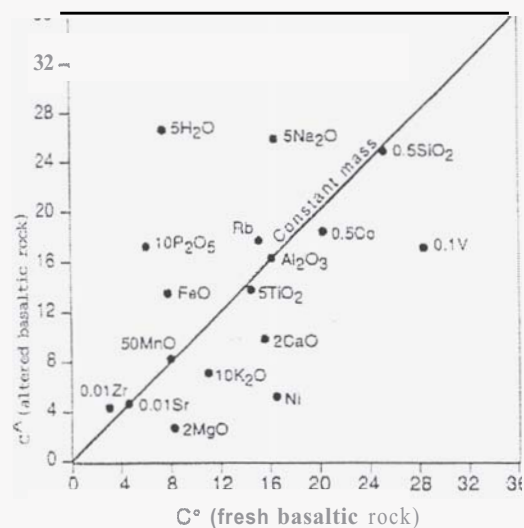


Figure 5. Comparison of components in the altered basaltic (Bofa basalt) core samples of 1050m (well LA-8) against those in the original basaltic (Bofa basalt) rock samples. Isocon diagram (Grant, 1986). Some rock chemical components whose concentrations are not accommodated comfortably are decreased/increased by a multiplying factor (e.g. 0.5 SiO<sub>2</sub> = 0.5 \* the SiO<sub>2</sub> content of the rock).

The geothermal fluids from wells LA-3, LA-6 and LA-8 contain <10, <14, <10 ppb of Au and <0.5, <0.5, 3.4 ppb of Ag respectively. Using thermodynamic data for gold aqueous species (Hayashi and Ohmoto, 1991), calculations indicate that LA-6 fluid is near saturation in gold, assuming the  $\text{HAu}(\text{HS})_2$  and  $\text{AuHS}^+$  complexes as dominant aqueous phases for gold (Teklemariam, 1996). Theoretical calculations indicate that the LA-8 fluid cannot carry this amount of gold to reach saturation. The preliminary conclusion could therefore be that the upflow zone of the field is a zone in which gold can be transported in solution whereas the more diluted and relatively cold water of LA-8 can deposit this metal. Significant amount of Ag has been found in the LA-8 water and the computed values of the saturation indices for silver and argentite are 4.1 and 8.1 respectively. These minerals are undersaturated in wells LA-3 and LA-6. Silver in well LA-8 is transported as chloride complexes, according to results of a computed species distribution.

## 9. CONCLUSIONS

Two types of alteration trends have been recognized using different chemical diagrams: argillic and propylitic. The samples from the lateral outflow zone show a pronounced alteration trend towards the phyllosilicate composition. This is in agreement with the common occurrence of chlorite, smectite, illite and other clay minerals in these rocks. On the other hand, a few samples show a different trend towards the calcite and epidote composition where a relict propylitic alteration is prominent in these rocks. The samples from the upflow zone depict alteration towards the calcite and epidote composition which is consistent with the propylitic alteration characterizing these rock samples. Preliminary data on the Ag and Au contents in the Aluto-Langano geothermal waters indicate that the water of well LA-6 could transport Au but not Ag, whereas Au could deposit in the zones of lateral outflow.

## 10. ACKNOWLEDGMENTS

This research work was financially supported by CNR (National Research Council of Italy). The author is grateful to the GSE for granting permission to publish the data. My grateful thanks are also extended to Ato Yohannes

Belete for his help in scanning and arranging figures.

## 11. REFERENCES

Electroconsult, ELC (1986). *Exploitation of Langano-Aluto geothermal Resources*, Feasibility report, Milan Italy.

Gizaw, B. (1989). *Geochemical investigation of the Aluto-Langano Geothermal field, Ethiopian Rift Valley*. MPH. Thesis (Unpubl). Dept of Earth Sci., Univ of Leeds. 237.

Grant, J. A. (1986). The Isocon diagram- A simple solution to Gresen's equation for metasomatic alteration. *Econ. Geology*, 81, pp. 1976-1982.

Hayashi, K.I. and Ohmoto, H. (1991). Solubility of gold in  $\text{NaCl}$  and  $\text{H}_2\text{S}$  bearing aqueous.solutions at 250-350°C. *Geochem. Comsmo. Acta*, 55, pp.2111 - 2126.

LA Roche, H de. (1975). Comportement geochemique differentiel de Na, K et Al dans les formations volcaniques et sedimentaire. *C. R. Acad. Sc. Paris*, 267, pp. 39-42.

Laury, R. L. and Albritton, C. Jr. (1975) Geology of middlestone age archeological sites in the Main Ethiopian Rift Valley. *Geol. Soc. Of Am. Bull.* 86, pp.999-1011

Mekuria, N., Gizaw, B., Teklu, A. and Gizaw, T. (1987). *Geochemistry of the Aluto-Langano geothermal field Ethiopia*. Ethiopian Institute of Geological Surveys, Internal Report, 1-55.

Teklemariam, M. (1996). *Water-rock interaction Processes in the Aluto-Langano geothermalfield, Ethiopia*. PhD. Thesis, Department of Earth Sciences, University of Pisa. 295.

Teklemariam, M., Battaglia, S., Gianelli G. And Ruggieri G. (1996): Hydrothermal Alteration in the Aluto-Langano Geothermal Field, Ethiopia. *Geothermics* Vol.25, No.6, pp. 679-702

Teklemariam, M. and Beyene, K. (2000; 2001). *Geochemical monitoring of the Aluto-Langano geothermal field, Ethiopia*. Internal report, GSE.

Wrinkler, H. G. F. (1974). *Petrogenesis of metamorphic rocks*, Third edition., New york Springer Verlag.